Journal of Sciences, Islamic Republic of Iran 24(3): 229-241 (2013) http://jsciences.ut.ac.ir
University of Tehran, ISSN 1016-1104

Some Aspects about Seismology of 2012 August 11 Ahar-Vaezaghan (Azarbayjan, NW of Persia) Earthquakes Sequences

M. Nemati*

Department of Geology, Faculty of Science, Shahid Bahonar University of Kerman, Kerman City, Islamic Republic of Iran
Earthquake Research Center, Physics Department, Shahid Bahonar University of Kerman, Kerman City, Islamic Republic of Iran

Received: 4 May 2013 / Revised: 19 June 2013 / Accepted: 18 July 2013

Abstract

In 2012 August 11 (12:23 UTC) a moderate earthquake with MW=6.4 (USGS) occurred between Ahar and Varzaghan towns in Azarbayjan Province at northwest of Iran. After eleven minutes another earthquake shook the area with MW=6.2 (USGS). These consecutive earthquakes followed by intensive sequences of aftershocks whereas the strongest one had MW=5.3 (USGS). In data processing including depth modification and focal mechanism solution, we used regional (Institute of Geophysics, University of Tehran (IGUT) and International Institute of Earthquake Engineering and seismology (IIEES) of Iran) and worldwide (ISC) seismological data. After processing westward fault propagation estimated using Building and House Research Center (BHRC) of Iran strong-motion records. Also depth of the mainshocks and some important aftershocks modified using pP phase travel times recorded with ISC stations (10-14 km) which are nicely situated in seismogenic part of crustal structure of the area. The focal mechanisms processed using first P motion method for the two mainshocks and dominant mechanisms calculated for the intense aftershocks (MN>4.0, IGUT) manifestly displayed a strike-slip movement on a steep south dipping nodal plane with near E-W strike without any interpretation using earthquakes location. These are associated with the Geological Survey of Iran (GSI) field observations.

Keywords: Earthquake; Focal mechanism; Aftershocks; Strike-slip and Steep dipping

Introduction

The 2012 August 11 Ahar-Vaezaghan earthquakes are situated in about 150 km distance from fast populated and mega city of Tabriz and also placed among many small to moderate cities in Azarbayjan, NW of Persia. Two tremors occurred consequentially in northeast of a historically [2] and recently [17] active fault system, North Tabriz Fault. During these earthquakes sequences 300 bodies missed, about 2500 people injured and about 150 villages damaged in a percentage range of 20-100 [3]. Surprisingly, the

* Corresponding author, Tel. / Fax: +983413222035, E-mail: majid_1974@uk.ac.ir

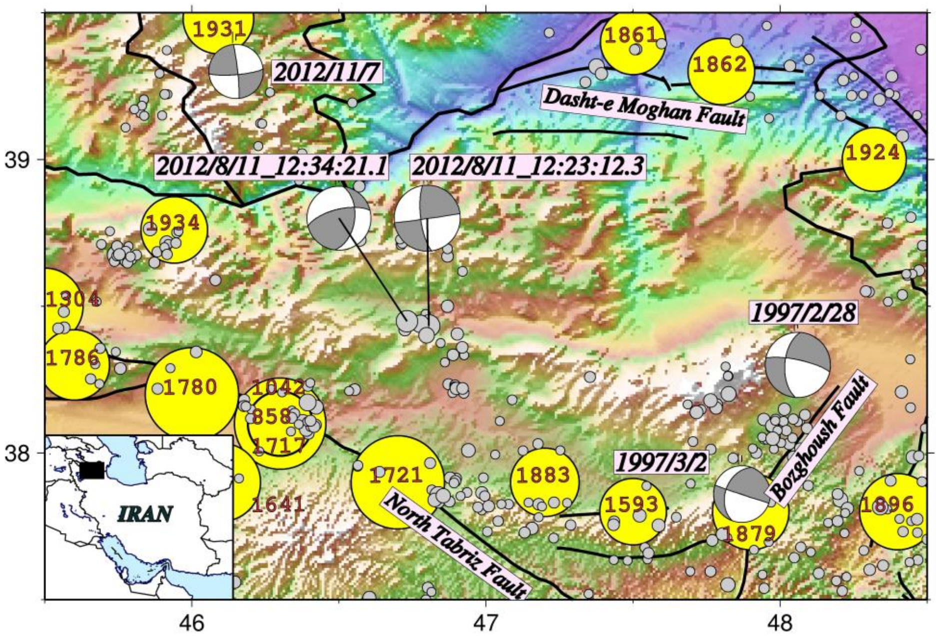

Figure 1. Regional seismotectonics map of the epicentral area of 2012 Ahar-Varzaghan earthquakes and around. Around area has experienced many historical earthquakes (adapted from Ambraseys and Melville, 1982 and Berberian and Yeats, 1999 [2, 28], yellow circles drawn with respect their magnitudes). Gray circles indicate IGUT recorded micro seismicity from 2006-2012 before strongly activation of the area. The focal mechanisms are from Harvard University [8] and the faults adapted from Hessami, et al., (2003a) [10].

epicentral area of the earthquakes neither experienced remarkable seismicity at the past centuries [2, 28] nor cut with a mapped and surveyed significant fault [1, 10, 33]. Some researchers pointed to a significant gap in historical seismicity at northwest of studied area [2]. Also active tectonics investigations illustrate that northwest of Iran is a potentially active area, regarding to 4-8 mmyear-1 rate of right-lateral strike-slip faulting [5], thrust and strike slip partitioning in Turkish Iranian Plateau [14] and counterclockwise rotation of the blocks

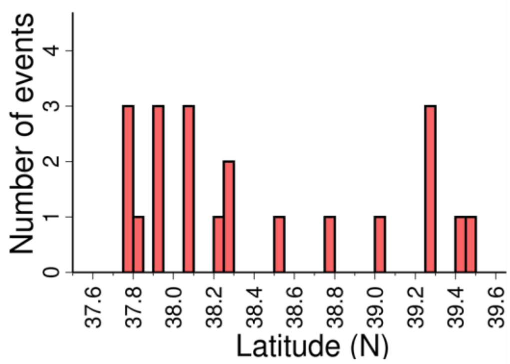

Figure 2. Histogram of historical and instrumental earthquakes occurred between 37.6-39.6°N in studied area. There is an earthquake gap between 38.3-39.2°N from 858 C.E. until present. See Fig.1.

in northwest of Iran bounded with right-lateral strike-slip faults [16]. The nearest (140 km further east) remarkable instrumentally earthquake (MW=6.0) to the study region occurred at 1997 in Ardebil area [5, 6]. In this paper which focuses on the greatest instrumentally earthquakes ever occurred at a poor seismically area (northwest of Persia), we used raw data of regional seismic networks of IGUT [12] and IIEES [13], global seismological data of ISC and strong motion data of BHRC [4]. Propose of this surveying is seismologically recognition of interacontinental earthquakes sequences which occurred in a seismically unknown area and explaining its correspondence with GSI [7] field geological beliefs [3] in the earthquakes affected area.

Seismotectonics and regional seismicity

The study area is a relay tectonically region between an active tectonic fault system, North Anatolian fault system located in Turkey, and the Alborz and Zagros in north and southeast of Iran respectively. The total shortening concluded from Arabia-Eurasia collision with a rate of 22 mm/year [26] across the NE Persia is partitioned into two fault systems, right-lateral strike-slip movements in the Turkish-Iranian Plateau like North Tabriz fault system and thrusting in the Caucasus [5]. In other word the study area is transferred a part of this Arabia-Eurasia northward relative motion to the

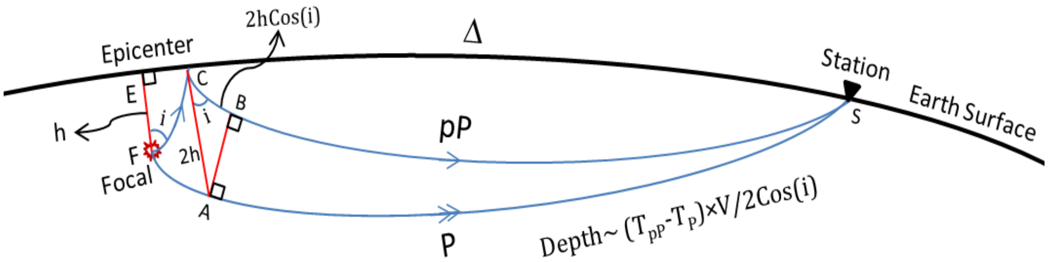

Figure 3. Schematic ray path drawn for pP for earthquakes with an epicentral distance (Δ) between 30°-90° [32]. In this picture FC=FA, CB= 2hCos(i), CA=2FE, T_{pP}-T_P=2hCos(i)/V.

Anatolia [16, 14]. Mason, et al., (2005) [15] measured 8 mm/year extension in 30°N direction in this area which is consistent with right-lateral strike-slip movements at the earthquake affected region.

In ancient countries like Persia with a rich history, it is expected that the historical earthquakes to be documented or at least explained descriptively in historical books (eg. Nasser Khosrau, 1052, the Book of Travel; Mas'udi, 943, Al-Tanbih val-Eshraf; Jovaini, 1260, The History of the World Conqueror) [31, 29, 30]. In this case, Iran is not an exception whereas around of the earthquake affected area experienced many significant historical and pre-instrumental earthquakes [2, 28]. Paleo-seismological investigations revealed that the North Tabriz fault system experienced at least 4 major destructive earthquakes during the past 3.5 ka [11, 24]. The area bounded with historical and a few instrumental earthquakes. Also a significant instrumentally earthquake occurred at the further east, where the mountains descend to meet western coast of the south Caspian Sea. There is a near N-S left-lateral strike-slip fault system which is the source of 1997/2/28 Ardebil earthquake [6] (Fig.1).

Materials and Methods

Data processing, including relocating the earthquakes of Table 1, performed using an exact crustal velocity structure. The velocity model calculated with inversion of travel times of microearthquake phases recorded with a dense local seismological network installed during 2004 [17]. In this paper we used the waveforms (including polarities) recorded with the seismological stations owned by IGUT [12], IIEES [13], ISC and accelerations recorded by stations owned by BHRC [4]. Also for magnitude investigation the 1298 aftershocks (MN> 2.5) recorded with IGUT network in two months were used. In this way we used first P motion method with SEISAN software [9] for focal mechanism solution and Generic Mapping Tools (GMT) software [27] for displaying the maps and the results. Propose of this surveying is seismologically recognition of interacontinental earthquakes sequences which occurred in a seismically unknown area and explaining its correspondence with GSI [7] field geological beliefs [3] in the earthquakes affected area.

Seismicity pattern

The Ahar-Varzaghan earthquakes occurred in an area which has experienced no significant historical and instrumental seismicity. As shown in Fig. 1, the epicentral area bounded with many historical earthquakes during 1154 years from 858 to 2012 C.E. In histogram of Fig. 2 which shows historical and instrumental earthquakes occurred between 45.5-49°E and 37.6-39.6°N, there is an obvious earthquake missing between 38.3-39.2°N. Consequently it could be supposed as a preparing seismological gap.

Depth modification

Focal depth of the mainshocks and some aftershocks were calculated using depth phases like pP and also P phase [32] recorded by the ISC stations (Table 1, Appen. 1 and 2 and Fig. 3). Actually the final depths presented in table 1 have been normally averaged between all of the stations. There is good correspondence between the depth calculated in this study and of the IGUT except 2012/08/11-19:52:43.4 and 2012/08/14-14:02:25.9 earthquakes. The depth range of the modified earthquakes placed between 9 and 14 km which are situated in seismogenic part of crustal structure [17] of the area.

Strong ground motion of the mainshocks

Iso-acceleration map of the 2012/08/11-12:23 and 12:34 earthquakes prepared using radial component of the strong-motion data recorded with the BHRC [4] stations [23] (Fig. 4 and 5). Maximum accelerations recorded with the Varzaghan station for first and second

Table 1. Source parameters of the mainshocks and the strongest aftershocks. The star marked (*) parameters were calculated in this paper.

Row	Orig. Time(GMT)	Long.(˚E)	Lat.(˚N)	Depth(km)	Depth(km)*	Mag.(M_N)	Nodal Plane(CMT)			Nodal Plane*		
							Strike˚	Dip˚	Rake˚	Strike˚	Dip˚	Rake˚
1	20120811-122315.3	46.806	38.433	9	10	6.2	175	81	6	187.61	55.61	-6.93
2	20120811-123434.8	46.798	38.401	10	12	6	10	50	36	178.66	45.7	-8.89
3	20120811-152114.5	46.789	38.428	14.2	-	4.5	-	-	-	6.88	80.15	-17.5
4	20120811-154319.2	46.735	38.436	9.7	11.8	4.8	-	-	-	172.27	75.97	32.4
5	20120811-195243.4	46.838	38.55	4	13.4	4.4	-	-	-	-	-	-
6	20120811-222402.0	46.759	38.482	4	-	4.8	254	89	149	182.9	58.68	60.35
7	20120813-015610.0	46.694	38.445	4.4	-	4.7	-	-	-	190.74	82.41	10
8	20120814-140225.9	46.789	38.454	6	12.4	5.3	-	-	-	54.98	54.06	86.29
9	20120815-174904.5	46.672	38.41	4	-	5	10	56	51	335	85	-5
10	20120816-171412.5	46.746	38.451	19.1	14	4.6	263	78	172	-	-	-
11	20120917-070547.0	46.675	38.46	4	-	4.1	-	-	-	166.83	90	35
12	20121008-082554.0	46.629	38.446	4	-	4.1	-	-	-	352.95	44.81	-35.53
13	20121016-041530.0	46.899	38.47	5.4	-	4.2	-	-	-	0.29	51.62	-12.25
14	20121026-223115.0	46.65	38.463	10	-	4.3	-	-	-	162.21	86.41	45.89
15	20121027-035641.9	46.648	38.396	4	-	4	-	-	-	220.95	41.49	79.4
16	20121107-062500.0	46.565	38.458	10	-	5.4	183	83	7	239.96	27.39	47.8
17	20121107-070100.0	46.591	38.45	4	-	4.1	-	-	-	10.72	31.47	16.74
18	20121108-094359.0	46.57	38.408	10	-	4.2	-	-	-	346.93	87.77	-47.96
19	20121110-135122.0	46.616	38.491	4	-	4	-	-	-	211.85	58.68	16.48
20	20121116-035425.0	46.57	38.48	10	-	4.7	199	89	9	261.67	36.05	52.49
21	20130303-205002.9	46.681	38.4	6.4	-	4.1	-	-	-	4.29	48.44	30.79
22	20130308 134542.0	46.676	38.367	4	-	4	-	-	-	49.49	49.45	45.81

mainshocks are 428 and 534 cm/s2 respectively (Appen. 3 and 4). According to GSI report, maximum intensity estimated about IV (in Mercalli modified scale) in longitude of 46.7° and a near E-W rupture with 15-20 km length mapped and documented [3] (black lines in Fig. 4 and 5). In both shocks, regarding to the stations situated in rupture strike, it is concluded that the area may ruptured from east to the west in a unilateral manner. The complete directivity effect could be calculated using duration of the strong-motion records, polarization of their components and the velocity pulses. Based on GSI field observations which performed a few days after mainshocks occurring, severely damaged villages during the earthquakes were situated near Varzaghan town in longitude of 46.65°. Along the co-seismic rupture from east to west, a gradually increase in damaging of the villages is manifestly seen at the area [3]. The villages with 100% damaging are placed in green and red areas in Fig. 4 and 5 respectively with near 350 cm/s2 acceleration. The western termination of the rupture in near maximum intensity confirms probable westward co-seismic fault propagation. Although the site effects on damaging should not be forgotten.

Magnitude of the aftershocks

The 2012 Ahar-Varzaghan earthquakes followed by numerous aftershocks. Number of 1298 aftershocks with the magnitude greater than 2.5 in MN scale [21] recorded with IGUT network in two months. The duration for investigated aftershocks is from 2012/08/11 to 2012/10/10.

Here, it is necessary explaining unique property of 2012/08/11-12:23 Ahar-Varzaghan earthquake. The earthquake sequences are different from the other intracontinental Persian earthquakes in number of the aftershocks and their magnitudes in a specific time range.

We have analyzed the time cumulative magnitude of the aftershocks versus time after the mainshock for Ahar-Varzaghan and 5 other large earthquakes (MN magnitude 5.0-6.4) occurred in Iran (Fig. 6). The aftershocks plotted during 60 days since mainshock with cut-off magnitude of 2.5 in MN scale. The slopes

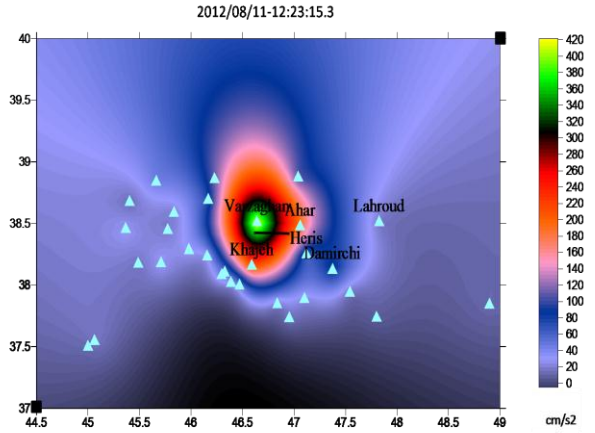

Figure 4. Iso-acceleration map of the 2012/08/11-12:23 earthquake drawn using radial component of the accelerations recorded with the BHRC [4] stations (light green triangles).

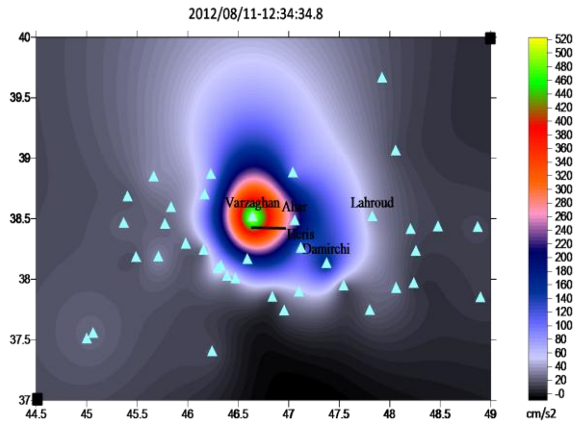

Figure 5. Iso-acceleration map of the 2012/08/11-12:34 earthquake prepared using radial component of the accelerations recorded with the BHRC [4] stations (light green triangles).

of these diagrams are characteristic of the co-seismic fault zones [1]. Also this could provide a useful way for understanding the temporal distribution of aftershocks after a specific mainshock. For a specific earthquake, the beginning of zero slop in this diagram indicates beginning of background seismicity which replaced with an aftershock sequence. Regarding to rise of the diagram drawn by inverse red triangles (Ahar in Fig. 6) and comparing it with diagrams of five Persian earthquakes, it could be concluded that the aftershock sequence of the Ahar-Varzaghan earthquake is much longer and almost 7 times intensive than the other large events. It is important that a reasonable comparison will only be achieved by using same database (IGUT) for the events.

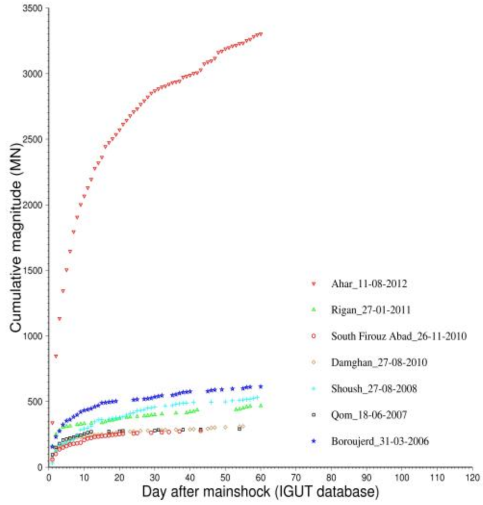

Figure 6. Plots of time cumulant of aftershocks magnitude for 7 Persian earthquakes versus number of days since their mainshocks using IGUT database [12].

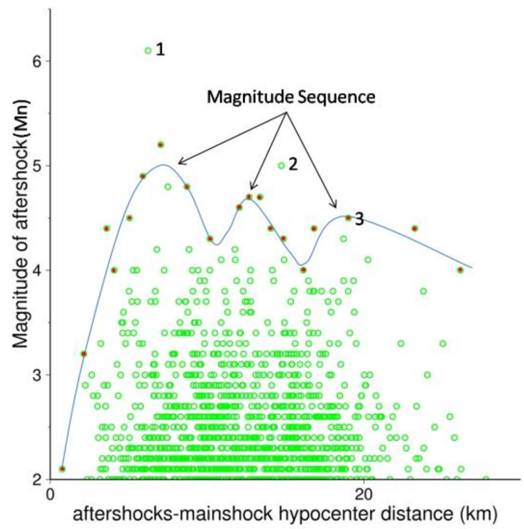

Figure 7. Relationship between aftershocks magnitude and the aftershock-mainshock hypocentral distance in 2012/08/11-12:23 Ahar-Varzaghan earthquake sequences. The circles are aftershocks occurred during 2 months following the mainshock. The red solid circles show largest aftershocks in approximate each 1-km interval of aftershock-mainshock hypocentral distance. The blue curve shows the smoothly curve fitting to the solid circles.

Figure 7 Shows the MN magnitude range of the aftershocks of August 11 Ahar-Varzaghan earthquake sequences versus their aftershock-mainshock hypocentral distances. In this picture the earthquake followed by sequences with three modal distributions. Each value of two minimums is one of the smallest values which separate the sequences. The aftershocks indicated by 1, 2 and 3 are the largest aftershocks in each aftershock sequences. The aftershock 3 is the furthest from the mainshock hypocenter. Its hypocentral distance to the mainshock could be reasonably assumed as co-seismic fault elongation of the earthquake at depth [18]. Therefore depth rupture length of the August 11 Ahar-Varzaghan (12:23) event estimated about 19 km. Thus the surface rupture must definitely have less elongation than 19 km (15-19 km in comparison with the GSI-report 15-20 km [3]).

Focal mechanism of the mainshocks and strongest aftershocks

The aftershocks plotted in map of Fig. 8 (red circles) occurred during less than three months. For better understanding of the earthquake source characteristics and co-seismic fault role in the seismotectonics regime of the area, we calculated 18 focal mechanisms for the mainshocks and the strongest aftershocks (#1-4, 6-9 and 11-20 with MN>4.0) and 2 events from background seismicity (#21 and 22) applying first P motion method on IGUT, IIEES and ISC polarities. Computing focal mechanisms of the earthquakes with regional phases using first P motion method is possible if any P phases (Capital P grapheme except pP) is used for polarity picking [19, 20, 22]. The visual characteristics of the focal mechanism of the earthquakes in the Fig. 8 are shown in Appen. 5. There is similarity between the strike, dip and rake of the nodal planes for the mechanisms calculated with Harvard University and this paper for #1. Also the USGS mechanism of #2 is look like to our obtained mechanism. The earthquakes #1-4, 6-9, 16 and 20 are situated in robust category (black) and the events # 11-15, 17-19, 21, and 22 have fair quality solution (gray). The events partitioning is clearly based on number of the polarities and their scattering in four quarters. The mechanisms #1-4, 7, 9, 11-14, 16-20 and 22 indicate right-lateral strike-slip movement associated with GSI near E-W mapped co-seismic faulting. From these events #1-3, 7, 9, 13, 16, 17, and 19 also indicate steep south dipping for the mentioned fault. Based on these mechanisms we definitely could not say anything about dip-slip component of the co-seismic rupture.

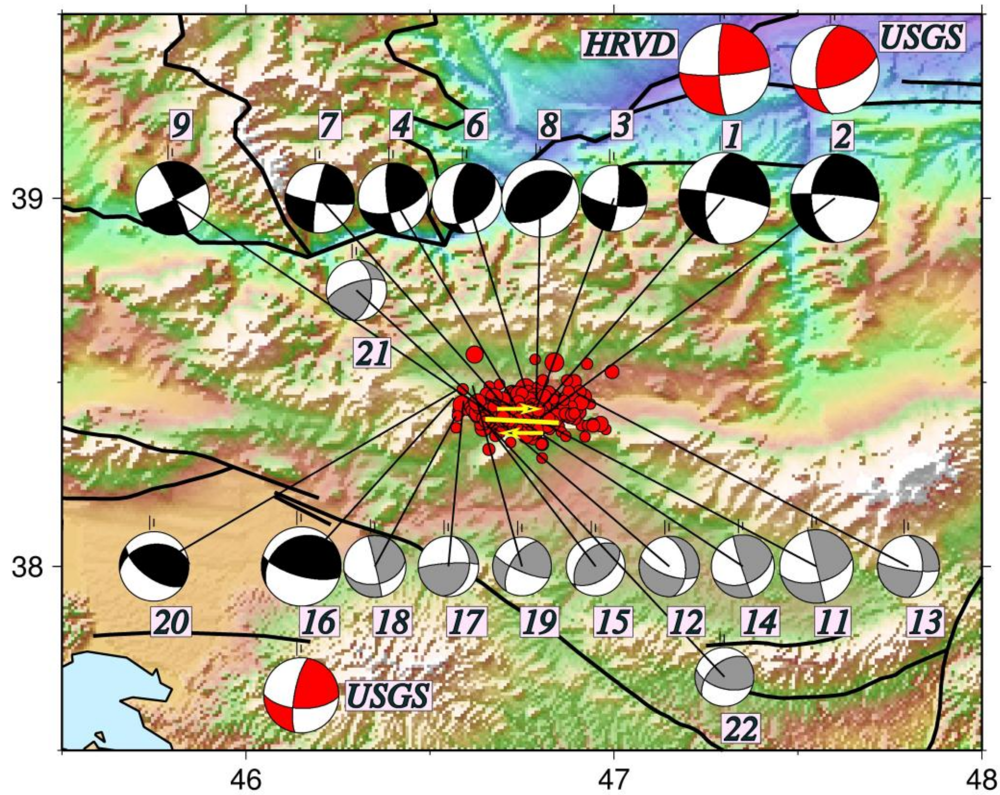

Figure 8. Focal mechanisms of the mainshocks and the greatest aftershocks. The red circles show IGUT recorded aftershocks, the red solutions adapted from global earthquake databases (like USGS [25] and Harvard University [9]) and the yellow thick line is GSI surveyed co-seismic rupture [3].

Results and Discussion

The 2012 Ahar-Varzaghan earthquakes occurred on a seismicity gap without any recognized and documented pre-existing fault which cut the epicentral area. This region is bounded with more than 20 large earthquakes in historical and instrumental period of time from 858 C.E. until present.

The modified depth range of some earthquakes is situated in seismogenic zone of the crust at the area. Focuses on strong motion data revealed a probable westward co-seismic fault propagation regarding to maximum acceleration recorded in western station and intense damaging of the villages in the west of the shook area. A length of about 19 km is estimated for earthquake rupture at depth which is in consistent with the field observations for surface rupture, 15-20 km. Regarding to that we do not present any interpretations

Appendix 1. The TGUT and IIEES seismological network stations used for processing of the focal mechanisms.

Symbol	Y(°N)	X(°E)	Z(m)	Organization	Symbol	Y(°N)	X(°E)	Z(m)	Organization
AFJ	35.856	51.7125	2750	IGUT	SAD	31.9136	53.6855	2457	IGUT
ANJ	35.4672	53.9144	2135	IGUT	SHI	29.6418	52.5133	1595	IGUT
ALA	36.0829	52.8099	2600	IGUT	SHV	37.5347	57.7027	1925	IGUT
AKL	36.6022	58.7566	2508	IGUT	SFB	34.3518	52.2406	948	IGUT
AZR	37.6783	45.98	2300	IGUT	SFR	37.0538	58	2448	IGUT
BAF	31.5902	55.5673	1485	IGUT	SRB	37.825	47.667	1950	IGUT
CHK	32.2442	54.4073	2030	IGUT	SHM	35.8067	53.2922	2500	IGUT
DHR	34.6997	46.3867	1434	IGUT	SRO	36.3088	59.4703	1050	IGUT
DMV	35.5772	52.0322	2546	IGUT	TBZ	38.2333	46.147	1650	IGUT
DAH	32.739	59.868	2277	IGUT	TEG	32.8965	58.7488	1745	IGUT
EMG	37.4155	58.6522	2565	IGUT	TBB	34.9954	51.7273	855	IGUT
FIR	35.6415	52.7536	2380	IGUT	TEH	35.7367	51.3817	1462	IGUT
FTB	38.0171	46.3944	2222	IGUT	RAZ	35.4046	49.929	1950	IGUT
GZV	36.3859	50.2184	2100	IGUT	RAM	31.8088	52.3815	2000	IGUT
GAR	32.4038	52.0418	2020	IGUT	VIS	34.5264	46.8496	1135	IGUT
GLO	36.5024	53.8302	1963	IGUT	VRN	34.9954	51.7273	855	IGUT
GHG	34.3294	46.5685	2090	IGUT	ZEF	32.8956	52.3291	2320	IGUT
HRS	38.3183	47.042	2100	IGUT	Shahrood (SHRD)	36	56.01	1264	IIEES
MHD	35.6853	50.6675	1150	IGUT	Maravetape (MRVT)	37.66	56.09	870	IIEES
MIN	37.2575	55.4069	180	IGUT	Ashtian (ASAO)	34.548	50.025	2217	IIEES
MAH	36.7666	45.7167	1344	IGUT	Persian Gulf (BNDS)	27.399	56.171	1500	IIEES
MEH	31.3902	54.613	2130	IGUT	Bojnurd (BJRD)	37.7	57.408	1337	IIEES
MRD	38.7133	45.703	1684	IGUT	Charan-Tehran(CHTH)	35.908	51.126	2350	IIEES
MOG	36.1082	59.3393	2577	IGUT	Damavand (DAMV)	35.63	51.971	2520	IIEES
MON	33.1922	59.6667	2150	IGUT	Germi-Ardebil (GRMI)	38.81	47.894	1300	IIEES
MHI	36.3088	59.4703	1150	IGUT	Ghir-Karzin(GHIR)	28.286	52.987	1200	IIEES
MYA	36.3416	60.1017	1684	IGUT	Ghom (GHVR)	34.48	51.295	927	IIEES
KRD	36.7759	59.5146	2245	IGUT	Kerman (KRBR)	29.982	56.761	2576	IIEES
KIA	36.207	53.6837	2167	IGUT	Khomeyn(KHMZ)	33.739	49.959	1985	IIEES
KLH	33.319	51.5787	2280	IGUT	Maku (MAKU)	39.355	44.683	1730	IIEES
KOO	32.4241	59.0044	2245	IGUT	Maravetape (MRVT)	37.659	56.089	870	IIEES
KOM	34.1745	47.5102	1502	IGUT	Naein (NASN)	32.799	52.808	2379	IIEES
IL3	35.4761	51.0238	989	IGUT	Sanandaj (SNGE)	35.093	47.347	1940	IIEES
IL5	35.2128	50.5811	1385	IGUT	Shooshtar (SHGR)	32.108	48.801	150	IIEES
LAS	35.3822	52.9589	2195	IGUT	Tehran (THKV)	35.916	50.879	1795	IIEES
PRN	36.2419	52.3381	1333	IGUT	Zahedan (ZHSF)	29.611	60.775	1575	IIEES
PIR	32.6841	50.8917	2600	IGUT	Zanjan (ZNJK)	36.67	48.685	2200	IIEES
PAY	36.45	58.996	2100	IGUT	Shahrakht (SHRT)	33.646	60.291	837	IIEES
PAR	29.8419	53.0485	2603	IGUT	Shahrood (SHRD)	36	56.01	1264	IIEES
QOM	34.8424	51.0703	2270	IGUT	Tabas(TABS)	33.649	57.119	-	IIEES
QAM	33.4564	51.1583	1790	IGUT	Ahram (AHRM)	28.864	51.295	80	IIEES
QHU	37.073	58.5394	1320	IGUT	Chabahar (CHBR)	25.28	60.6	125	IIEES
SHB	38.2833	45.617	2150	IGUT	Mashhad (MSHD)	36.587	59.943	1965	IIEES
SRV	29.3817	53.1133	2688	IGUT					

Appendix 2. The ISC stations used for depth modification using pP phase travel time.

Symbol	X(° ´)	Y(° ´)	Z(m)	Organization
MORC	4946.61N	1732.55E	743	ISC
ARCES	6932.09N	2530.35E	403	ISC
SPITS	7810.66N	1622.20E	323	ISC
FINES	6126.62N	26 4.63E	150	ISC
SUMG	7234.58N	3827.23W	3275	ISC

Appendix 3. Accelerations recorded with BHRC accelerometry network stations for the 2012/08/11-12:23 earthquake.

Acceleration(cm/s2)			Coordinate		Station	Row
T	V	L	Lat.(°N)	Long.(°E)		
373	248	428	38.507	46.64	Varzaghan	1
281	97	216	38.154	46.589	Khajeh	2
261	100	193	38.474	47.059	Ahar	3
98	40	58	38.247	47.119	Heris	4
86	47	92	38.123	47.373	Damirchi	5
83	52	72	38.688	46.166	Kharvanagh	6
80	39	111	38.86	46.229	Dozal	7
60	69	104	38.87	47.039	Kaleibar	8
50	18	45	38.839	45.662	Hadi Shahr	9
39	19	49	38.102	46.327	Tabriz1	10
48	29	38	37.996	46.471	Basmenj	11
32	22	26	38.017	46.388	Tabriz2	12
28	20	45	38.078	46.298	Tabriz3	13
20	11	29	38.176	45.708	Shabestar	14
20	11	18	38.585	45.834	Zonouz	15
19	11	15	38.507	47.826	Lahroud	16
17	10	11	37.935	47.541	Sarab	17
17	12	17	38.445	45.774	Marand	18
16	7	15	37.731	46.953	Tikmah Dash	19
16	12	29	38.456	45.366	Zanjir	20
15	9	23	38.231	46.156	Amand	21
13	15	22	37.887	47.101	Sharbian	22
13	7	6	37.734	47.801	Avin	23
12	7	14	37.846	46.837	Bostan Abad	24
12	10	11	38.672	45.403	Yekan Kahriz	25
10	6	16	37.544	45.063	Oroumieh	26
9	3	10	37.839	48.897	Talesh	27
9	3	10	37.498	44.999	Band	28
5	10	14	38.174	45.487	Sharafkhaneh	29
3	13	30	38.284	45.98	Soufian	30

based on the earthquake locations, the focal mechanism solution concluded a near E-W elongation, strike-slip and right-lateral motion and steep south dipping for co-seismic fault plane associated with surface geological surveying.

Acknowledgment

Hereby we thanks to the Institute of Geophysics, University of Tehran and International Institute of Earthquake Engineering and seismology of Iran for providing seismological data and thanks to Building and House Research Center of Iran for preparing the strong motion records.

Appendix 4. Accelerations recorded with BHRC accelerometry network stations for the 2012/08/11-12:34 earthquake.

Acceleration(cm/s2)			Coordinate		Station	Row
T	**V**	**L**	**Lat.(°N)**	**Long.(°E)**		
532	215	534	38.507	46.64	Varzaghan	1
420	204	238	38.474	47.059	Ahar	2
193	87	168	38.123	47.373	Damirchi	3
240	82	160	38.154	46.589	Khajeh	4
269	73	105	38.247	47.119	Heris	5
110	91	103	38.87	47.039	Kaleibar	6
69	42	80	38.86	46.229	Dozal	7
70	61	68	38.688	46.166	Kharvanagh	8
57	43	66	38.078	46.298	Tabriz1	9
43	19	51	38.102	46.327	Tabriz2	10
37	24	44	37.887	47.101	Sharbian	11
43	23	42	37.996	46.471	Basmenj	12
31	20	36	38.507	47.826	Lahroud	13
32	26	35	38.017	46.388	Tabriz3	14
29	14	33	38.839	45.662	Hadi Shahr	15
16	12	32	38.176	45.708	Shabestar	16
26	11	26	38.585	45.834	Zonouz	17
21	13	22	38.284	45.98	Soufian	18
27	6	22	37.918	48.062	Kerigh	19
20	7	22	37.544	45.063	Oroumieh	20
16	5	21	37.498	44.999	Band	21
17	11	21	38.231	46.156	Amand	22
18	11	21	38.456	45.366	Zanjir	23
21	13	20	38.445	45.774	Marand	24
31	16	19	37.734	47.801	Avin	25
18	5	18	39.655	47.924	Pars Abad	26
18	9	16	37.731	46.953	Tikmah Dash	28
11	6	15	38.403	48.206	Taleb Gheshlaghi	29
13	11	15	38.672	45.403	Yekan Kahriz	30
5	10	14	38.174	45.487	Sharafkhaneh	31
11	6	14	37.396	46.24	Maragheh	32
17	6	13	39.05	48.057	Germi	33
10	4	12	38.422	48.869	Astara	34
17	10	11	37.935	47.541	Sarab	35
10	4	11	38.423	48.477	Namin	36
9	4	10	38.222	48.258	Ardebil	37
10	2	9	37.839	48.897	Talesh	38
11	7	7	37.846	46.837	Bostan Abad	39
13	4	7	37.957	48.237	Kouraeim	40

Appendix 5. Visual characteristics for computed focal mechanisms.

1)

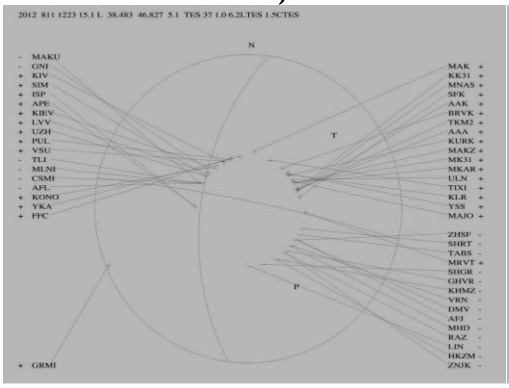

2)

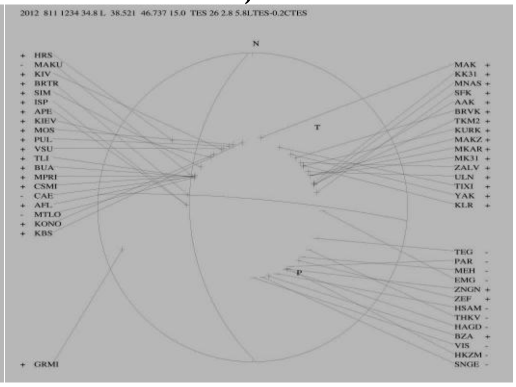

3)

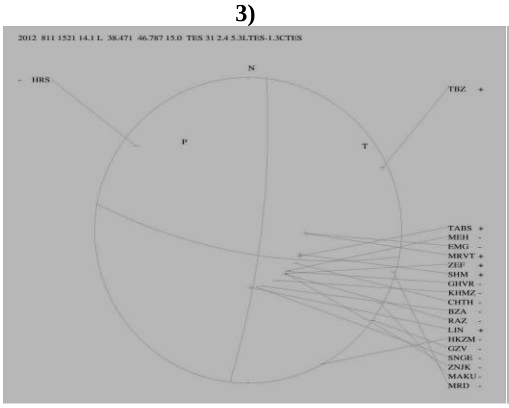

4)

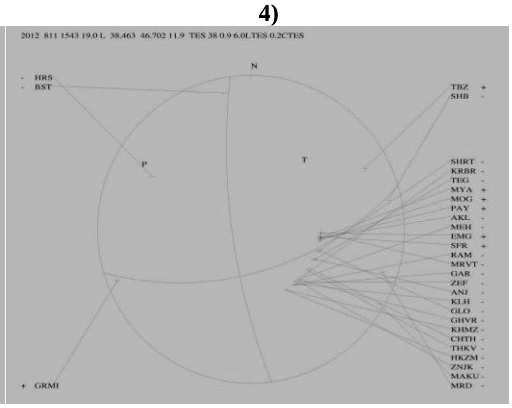

6)

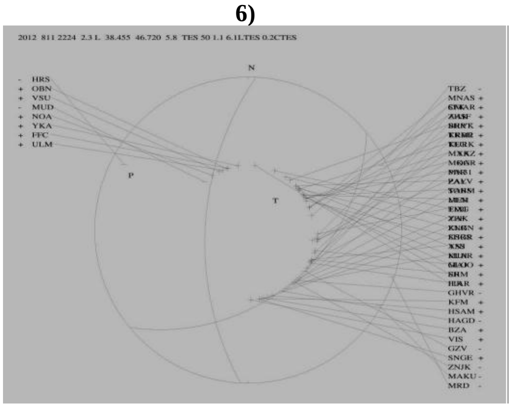

7)

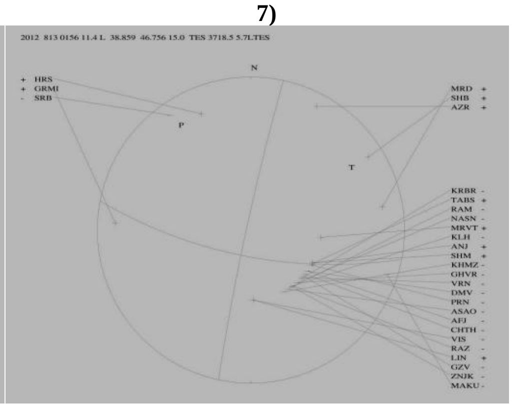

8)

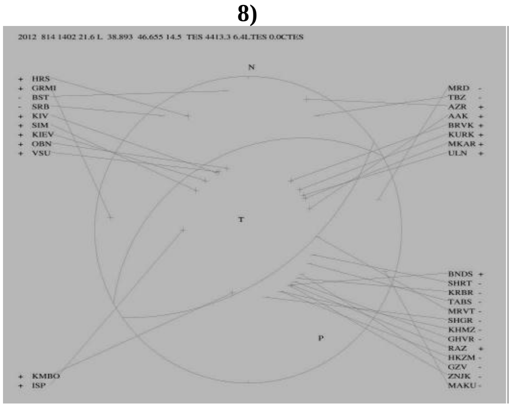

9)

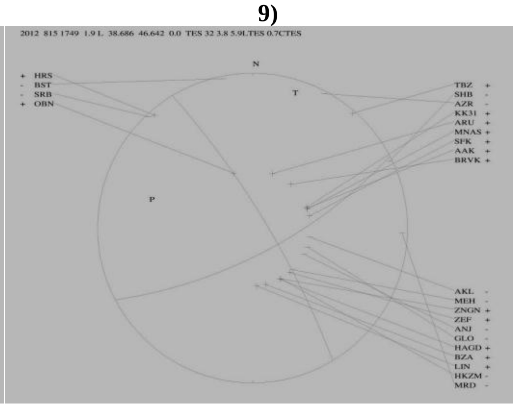

11)

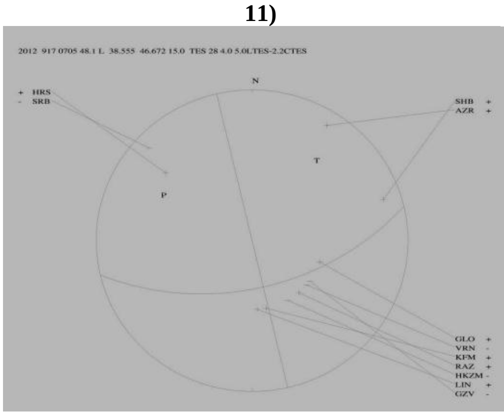

12)

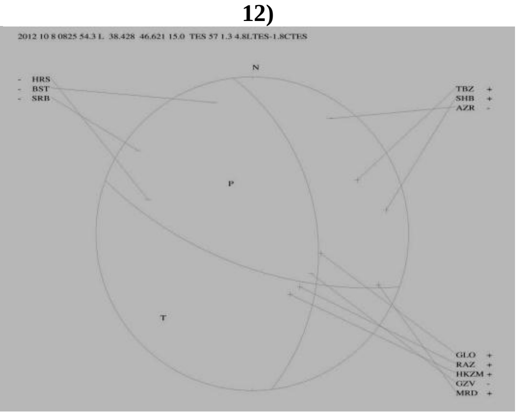

13)

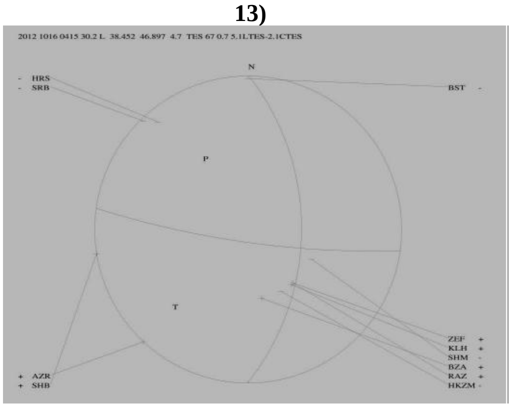

14)

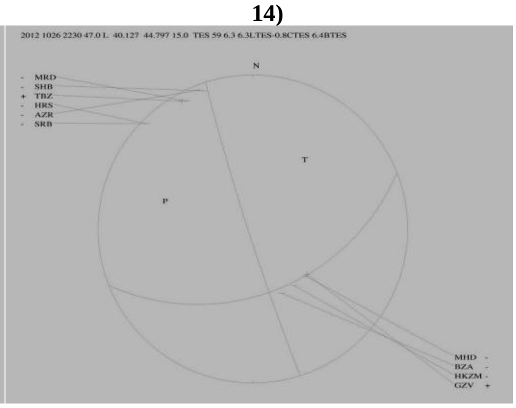

15)

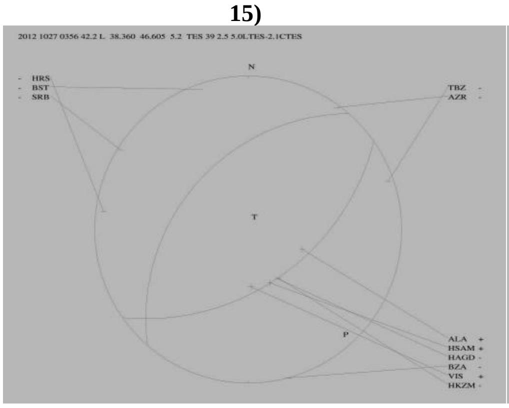

16)

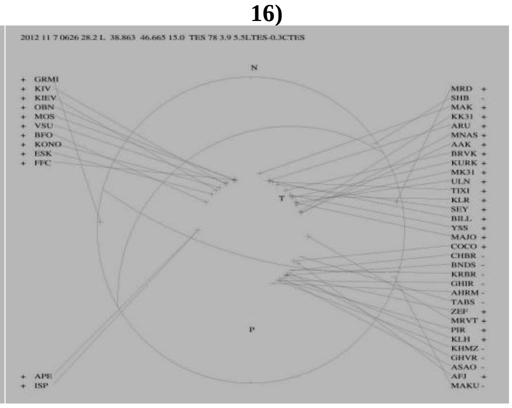

17)

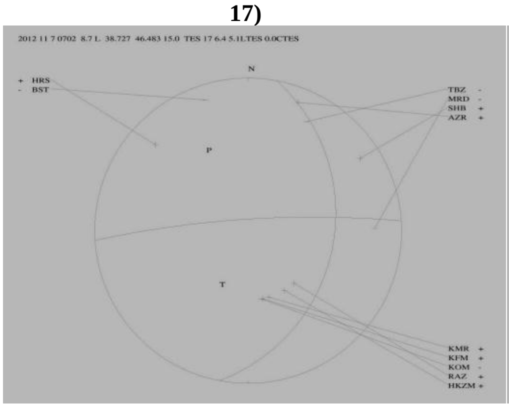

18)

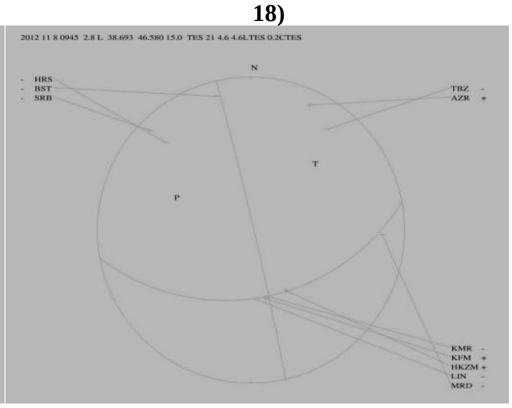

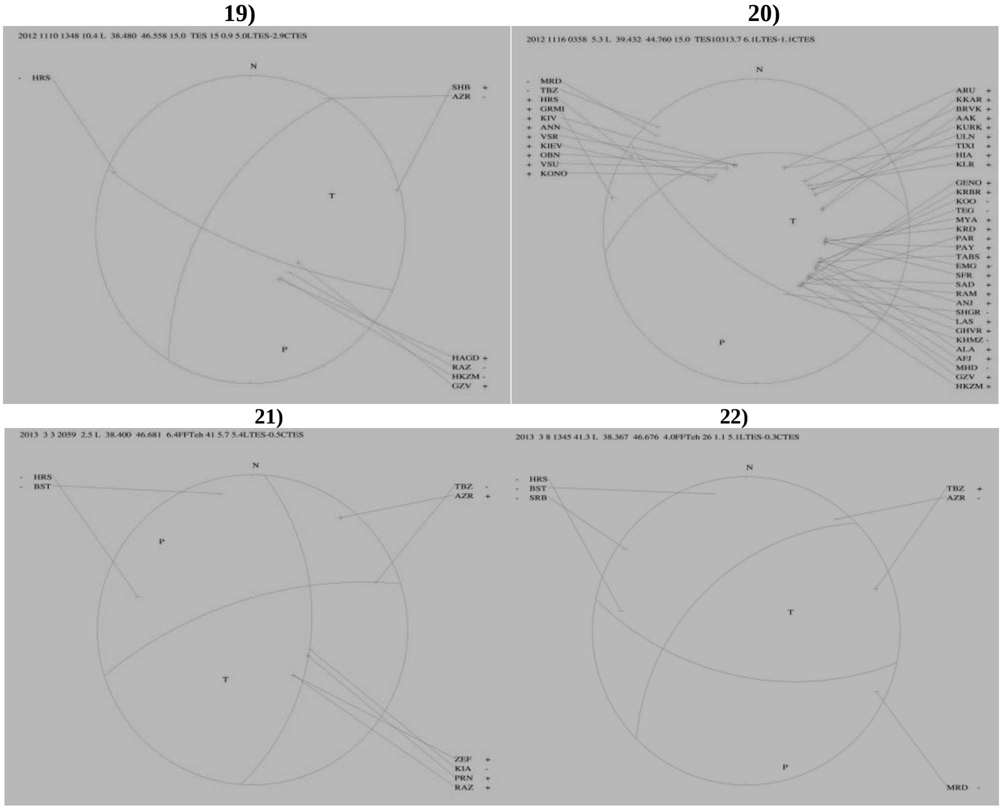

References

1. Bhattacharya P., Bikas K. and Chakrabarti K. The time distribution of aftershock magnitudes, fault geometry and aftershock prediction. Princeton University press, Available from: arxiv.org ,10/2009; DOI: abs/0910.3738 (2009).
2. Berberian M. and Yeats R. Patterns of Historical Earthquake Rupture in the Iranian Plateau. *BSSA*, **89**:120–139 (1999).
3. Bolourchi M-J., Solaymani Azad S., Faridi M., Oveisi B., Ghalamghash J. and Sartipi N. Preliminary report of 2012 Aug. 11 Ahar-Varzaghan earthquake, NE Iran. *Geological Survey of Iran (GSI),* internal report (in Persian), http://www.gsi.ir (2012).
4. Building and House Research Center (BHRC) accelerometry network, http://www.bhrc.ac.ir.
5. Copley A. and Jackson J. Active tectonics of the Turkish-Iranian Plateau. *Tectonics,* 25, TC6006. doi:10.1029/2005TC 001906 (2006).
6. Gheitanchi M-R and Bayramnajad E. The February 28, Ardabil, North-West Iran, Earthquake and its aftershocks. *Journal of Earth and Space Physics*, 24:Nos., 1 and 2 (1998), 1-9 (1998).
7. Geological Survey of Iran. GSI, http://www.gsi.ir.
8. Harvard University earthquake catalogue. Department of Geological Sciences, Centroid Moment Tensor catalogue, http://www.seismology.harvard.edu/CMTsearch.html.
9. Havskov J. and Ottemöller L. SEISAN: the earthquake analysis software, version 8.1, http://www.geo.uib.no/Seismologi/SOFTWARE/SEISAN_8.1/ (2005).
10. Hessami K., Jamali F. and Tabassi H. Map of Major Active Faults of Iran, Tech. rep., *International Institute of Earthquake Engineering and Seismology of Iran (IIEES),* http://www.iiees.ir (2003a).
11. Hessami K., Pantosti D., Tabassi H., Shabanian E., Abbassi M-R., Feghhi K. and Solaymani S. Paleoearthquakes and slip rates of the North Tabriz Fault, NW Iran: preliminary results. *Annals of Geophysics,* 46:903–915 (2003b).
12. Institute of Geophysics University of Tehran, *IGUT,* http://irsc.ut.ac.ir.
13. International Institute of Earthquake Engineering and Seismology, *IIEES,* http://www.iiees.ac.ir.
14. Jackson J. Partitioning of strike-slip and convergent motion between Eurasia and Arabia in Eastern Turkey and the Caucasus. *JGR,* **97**: (12), 471– 12479 (1992).
15. Masson F., Ch´ery J., Hatzfeld D., Martinoid J., Vernant P., Tavakoli F. and Ghafoury Ashtiani M. Seismic versus aseismic deformation in Iran inferred from earthquakes and geodetic data. *GJI,* **160**: 217–226 (2005).
16. McKenzie D.P. Active tectonics of the Mediterranean region. *GJR,* **30**:109–185 (1972).
17. Moradi-S. A., Hatzfeld D. and Tatar M. Microseismicity and seismotectonics of the North Tabriz fault (Iran). *Tectonophysics,* **506**: 22-30 (2011).
18. Nanjo K. and Nagahama H. Observed correlations

between aftershock spatial distribution and earthquake fault lengths. *Terra Nova,* **12**(6): 312–316 (2000).
19. Nemati M., Hollingsworth J., Zhong W., Bolourchi M-J. and Talebian M. Micriseismicity and seismotectonics of the South Caspian Lowlands, northeast of Iran. *GJI,* doi: 10.1093/gji/ggs114 (2013).
20. Nemati M., Hatzfeld D., Gheitanchi M., Sadidkhouy A. and Mirzaei N. Microseismicity and seismotectonics of the Astaneh-Firuzkuh faults at eastern Alborz, Iran. *Tectonophysics,* **506** (2011): 11-21 (2011).
21. Nuttli O. W. Seismic wave attenuation relations for eastern North America. *JGR,* **78**: 876–855 (1973).
22. Ottemöller L. and Havskov J. SEISAN: The earthquake analysis software, version 9.1, http://www.geo.uib.no/Seismologi/SOFTWARE/SEISAN_9.1/ (2012).
23. Rezapour M. Analysis of the causative fault during Silakhour earthquake, March 31, 2006 in Lorestan province. *Iranian Journal of Geophysics,* **3**(1):75-89 (2007).
24. Solaymani Azad S., Dominguez S., Philip H., Hessami K., Forutan M-R., Shahpasand Zadeh M. and Ritz J-F. The Zandjan fault system: Morphological and tectonic evidences of a new active fault network in the NW of Iran. *Tectonophysics,* **506** (2011): 73–85 (2011).
25. United State Geological Survey, USGS, http//:www.neic.usgs.gov.
26. Vernant P., Nilforoushan F., Hatzfeld D., Abassi M., Vigny C., Masson F., Nankali H., Martinod J., Ashtiani A., Bayer R., Tavakoli F. and Che´ry J. Contemporary crustal deformation and plate kinematics in Middle East constrained by GPS measurements in Iran and northern Oman. *GJI.,* **157**: 381–398 (2004).
27. Wessel P. and Smith W. H. F. New improved version of Generic Mapping Tools released. EOS, Trans. *AGU,* **79** (47): 579 (1998).
28. Ambraseys N. and Melville C. A., *History of Persian Earthquakes.* Cambridge University Press (1982).
29. Jovaini. *The History of the World Conqueror*, J. A. Boyles (Translator), 2 Vols., Manchester, U.K., 1958 (1260).
30. Mas’udi. *The Admonishment and Knowledge (Al-Tanbih val-Eshraf), translated into Persian by Abolqllasem Payandeh,* republished by Bongah Tarjomeh va Nashr Ketab Publ. Tehran, 1986 (in Persian) (943).
31. Nasser Khosrau. *The Book of Travel, Travel Diary of Naser Khosrau (Safarnameh),* republished 1976 in Tehran, Mohammad Dabir Siyaqi (Editor), 198 pp. (in Persian) (1052).
32. Stein S. and Wysession M. *An Introduction to Seismology, Earthquakes and Earth Structure.* ISBN 0-86542-078-5 (2003).
33. Solaymani Azad S. Evaluation de l'aléa sismique pour les villes de Téhéran, Tabriz et Zandjan dans le NW de l'Iran. Approche morphotectnique et paléosismologique, *PhD thèses de l'Université de Montpellier 2.* 150 pp (2009).